



Evaluation of physiological strain in hot work areas using thermal imagery

Clint A. Holm*, Leon Pahler, Matthew S. Thiese, Rodney Handy

Rocky Mountain Center for Occupational and Environmental Health, Department of Family and Preventative Medicine, School of Medicine, University of Utah, Salt Lake City, UT, USA

ARTICLE INFO

Article history:

Received 8 June 2016

Received in revised form

15 July 2016

Accepted 15 July 2016

Available online 16 July 2016

Keywords:

Heat strain

Heat stress

Core temperature

Physiological strain index

Hot work

Thermal imaging

ABSTRACT

Background: Monitoring core body temperature to identify heat strain in workers engaged in hot work in heat stress environments is intrusive and expensive. Noninvasive, inexpensive methods are needed to calculate individual Physiological Strain Index (PSI).

Objective: Thermal imaging and heart rate monitoring were used in this study to calculate Physiological Strain Index (PSI) from thermal imaging temperatures of human subjects wearing thermal protective garments during recovery from hot work.

Methods: Ten male subjects were evaluated for physiological strain while participating in hot work. Thermal images of the head and neck were captured with a high-resolution thermal imaging camera concomitant with measures of gastrointestinal and skin temperature. Lin's concordance correlation coefficient (ρ_c), Pearson's coefficient (r) and bias correction factor (C_b) were calculated to compare thermal imaging based temperatures to gastrointestinal temperatures. Calculations of PSI based thermal imaging recorded temperatures were compared to gastrointestinal based PSI.

Results: Participants reached a peak PSI of 5.2, indicating moderate heat strain. Sagittal measurements showed low correlation ($\rho_c=0.133$), moderate precision ($r=0.496$) and low accuracy ($C_b=0.269$) with gastrointestinal temperature. Bland-Altman plots of imaging measurements showed increasing agreement as gastrointestinal temperature rose; however, the Limits of Agreement (LoA) fell outside the ± 0.25 C range of clinical significance. Bland-Altman plots of PSI calculated from imaging measurements showed increasing agreement as gastrointestinal temperature rose; however, the LoA fell outside the ± 0.5 range of clinical significance.

Conclusion: Results of this study confirmed previous research showing thermal imagery is not highly correlated to body core temperature during recovery from moderate heat strain in mild ambient conditions. Measurements display a trend toward increasing correlation at higher body core temperatures. Accuracy was not sufficient at mild to moderate heat strain to allow calculation of individual physiological stress.

© 2016 Elsevier Ltd. All rights reserved.

1. Introduction

Heat stress is the heat load a worker is exposed to and is composed of environmental factors (such as air temperature, humidity, air velocity and radiant heat), metabolic heat, and clothing and Protective Personal Equipment (PPE) factors. Heat strain is the individual physiological response to heat stress. Heat strain as a response to heat stress is highly variable in individuals, with factors such as underlying health, acclimation, lifestyle and genetics affecting the occurrence of heat stress disorders (Nagano et al., 2010). High heat stress may lead to

high heat strain, potentially resulting in a number of heat related illnesses including heat stroke, which is life threatening. During the 2-year period covering 2012–2013, 20 cases of heat illness or death involving 18 private employers and two federal agencies produced citations for lack of federal OSHA enforcement. Thirteen of these cases resulted in a worker's death and two or more employees experienced symptoms of heat illness in seven of the cases (Arbury et al., 2014).

Heat stress resulting from exposure and worker exertion within hot workplace environments is common in many occupational groups, including smelter workers. The increased risk of heat strain in these occupational groups means that early and accurate detection and mitigation of physiological strain is essential for protecting the health of these workers (American Conference of Governmental Industrial Hygienists, 2015).

* Corresponding author.

E-mail address: clint.holm@utah.edu (C.A. Holm).

There are three types of thermal strain indices currently in use (Parsons, 1999):

- Environmental indices measure ambient heat stress, which may be used as an indicator for potential heat strain among workers. Currently used environmental indices include the American Conference of Governmental Industrial Hygienists (ACGIH) Threshold Limit Value (TLV) Screening Threshold, Occupational Safety and Health (OSHA) Heat Index and Wet Bulb Globe Temperature (WBGT).
- Thermoregulatory heat transfer models such as the ACGIH TLV Detailed Analysis include clothing/PPE and metabolic rate adjustments, which may be used to evaluate the potential for heat strain among Similarly Exposed Groups (SEGs).
- Physiological models such as the Physiological Strain Index (PSI) provide individual, real-time estimates of heat strain (Moran et al., 1998).

Real-time monitoring of PSI in occupational settings is currently limited due to the intrusive nature of gathering core temperature measurements, which requires use of a rectal temperature probe or ingestion of an intestinal telemetry temperature sensor (hereafter referred to simply as sensor) to measure rectal or gastrointestinal temperature, respectively. Due to these limitations, thermal indices are the primary control measure used in hot work environments. However, due to individual variability among workers, thermal indices are designed to be conservative and may unnecessarily restrict work as a result. A less intrusive method for monitoring core body temperatures for PSI calculation would allow monitoring and detection of individual heat stress response before the worker experiences symptoms of heat strain.

Research by Bourlai et al. (2012) used thermal imaging of the skin of the head and neck to estimate body core temperatures of participants before, during, and after treadmill exercise in a heated room with participants wearing wild land firefighting garments. The estimated body core temperatures showed a strong correlation with GI temperature during exertion within a heated enclosure, with a bias of only -0.07°C (1.4°C). However, the results of this research have not been confirmed in an occupational setting.

Thermal imagery may prove useful in rapid screening when used for determination of core temperature immediately upon cessation of hot work. Therefore, the use of thermal imagery of the skin of workers in comparison to gastrointestinal temperature for evaluation of physiological strain in hot occupational environments was investigated during this study. Although studies like that of Bourlai et al. are useful in establishing a correlation between thermal imaging and body core temperatures, the work of investigating, validating, and establishing such correlations in an actual occupational setting remains undone. The goal of this project was to validate the use of thermal imagery temperatures of the skin of workers in comparison to gastrointestinal temperature for evaluation of physiological strain in a real-world occupational setting.

2. Material and methods

Inclusion of human participants in this study was approved by the University of Utah Institutional Review Board (IRB; Approval #00082999). Prior to enrolling participants in the study, written informed consent for the pre-study questionnaire, monitoring for the study, and a post-sampling questionnaire were obtained.

2.1. Study design and participant recruitment

This cross-sectional study investigated the evaluation of physiological strain using thermal imaging of the skin of the head and neck of smelter and foundry workers rather than rectal or intestinal temperature in hot occupational environments. The study location consisted of a copper smelter located in the western United States. The site was selected for the hot work environment and work activities that necessitate thermal protective clothing.

The study population consisted of copper smelter furnace tappers. These tappers work rotating 12-h shifts on a 28-day schedule and are responsible for opening, maintaining and closing furnace holes as needed to control blister and matte copper levels within the furnace. Tapper PPE includes nonflame resistant coveralls, Nomex[®] arm sleeves, Nomex[®] hood, aluminized leathers, helmet, face shield, aluminized hood and full face respirator; all of which decrease the efficiency of the body's natural thermal compensation through evaporation of sweat. Work is production driven, but self-paced and a sufficient number of employees are on duty for tappers to rotate as necessary based upon workers' perceived exertion. Tappers are provided climate-controlled rest areas for recovery. Employee interviews indicated hot work periods vary from 30 min to several hours depending upon furnace hole conditions. Ambient conditions within the work area are variable and highly dependent upon external environmental conditions. At the time of sampling, ambient conditions were qualitatively judged by the tappers to be mild. According to the nearest National Weather Service station, seasonal highs ranged from 4 to 13°C , lows ranged from -6 to 5°C , and average relative humidity was between 54% and 86%. However, due to the high temperatures of the molten copper—in excess of 1200°C —temperatures at tapper work positions exhibited a strong gradient and were significantly above ambient conditions. Additionally, the tappers were exposed to high levels of infrared radiation, which is known to contribute to thermal load.

The primary participant inclusion criterion was current employment as a copper furnace tapper. Exclusion criterion was potential contraindications associated with the ingestion of the sensor. Recruitment took place in the smelter's work center and being included in the study was entirely voluntary. Participants were not provided with any incentives, but still received their regular rate of pay.

After obtaining a participant's informed consent as required by the IRB, a self-administered questionnaire was given to evaluate eligibility and obtain a brief medical history. Questions concerning potential contraindications associated with the ingestion of the sensor (i.e., gastrointestinal surgery, felinization of the esophagus, esophageal stricture, hypomotility disorders, etc.) were evaluated by a physician associated with the study. No contraindications were reported, therefore, no physician clearances were required. Self-reported demographic information was captured including age, weight, height, sex, time of gastrointestinal thermometer ingestion, smoking history, and exercise frequency. The median age was 40.7 years. The median height was 178 cm with a median weight of 98 kg, yielding a median BMI of 30.8. Participants reported a median frequency of 3.0 aerobic and 2.7 strength sessions per week. Current smokers represented 30% of the participants, while 30% were former smokers and the remaining 40% had never smoked. None had consumed alcohol within 24 h of reporting to work. While demographic information was not utilized in the analysis, it is crucial for describing the participant population. Demographic characteristics of the participants are found in Table 1.

Following completion of the questionnaire, participants were instructed to refrain from consuming alcohol for 24 h prior to the study-monitoring period. During monitoring potential

Table 1
Participant characteristics. Values are expressed as mean (\pm standard deviation).

Age (years)	Weight (kg)	Height (cm)	BMI	Aerobic Frequency (weekly)	Strength Frequency (weekly)
40.7 (\pm 9.9)	98 (\pm 18)	178 (\pm 6.5)	30.8 (\pm 4.7)	3.0 (\pm 1.4)	2.7 (\pm 1.0)

interferences were noted, such as: cigarette breaks and food and liquid consumption. After monitoring the participants were instructed to complete a final, post-sampling questionnaire. This self-administered questionnaire assessed recent consumption of alcohol, caffeine, and prescription medication use along with a personal evaluation of the previous night's sleep, the current work-day, and participant's mood.

One female and 13 male participants were initially recruited. The female participant was not monitored due to job reassignment, 2 males failed to ingest the intestinal telemetry pill as required and 1 male voluntarily withdrew from the study. The remaining 10 male participants were sampled on 5 separate days over a 5-week period in November and December 2015. Six of the 10 participants were continuously measured at 20-s intervals for gastrointestinal temperature and heart rate over the full shift. Due to the limited number of available data recorders, the remaining 4 participants were measured only when thermal imagery was performed.

2.2. Measurement methods

While PSI is the current gold standard in measuring heat strain, both rectal and gastrointestinal temperature used in PSI calculation are known to have long-term stability due to thermal inertia. Rectal temperature response phase delays of up to 60 min have been observed (Taylor et al., 2014). A combination of heat stress and exercise may lead to reductions in visceral blood flow, resulting in increased phase delays (Taylor et al., 2014), and this may potentially lead to incorrect PSI readings. It is hypothesized that alternate measures of body temperature may be more reactive to heat stress and thereby provide a more dynamic and accurate index of physiological strain.

To these ends, the following physical parameters were measured:

- Maximum Frontal Skin (MFSK) temperature.
- Maximum Side Skin (MSSK) temperature.
- Superficial Temporal Artery (STA) temperature.
- Posterior Auricular Artery (PAA) temperature.
- Gastrointestinal (GI) temperature.
- Heart Rate (HR).

Maximum skin temperature was measured by a Fluke Ti45FT-10/20 mid-wave infrared thermal imaging unit (Fluke Corporation, Everett, Washington). The instrument utilizes vanadium oxide microbolometers in a 160×140 focal plane array, yielding a thermal sensitivity of ≤ 0.08 °C in the 8–14 μ m spectral band. For MFSK measurements, the imaging unit was positioned to maximize the head and neck in the imaging frame and was perpendicular to the coronal plane. For MSSK measurements, the imaging unit was positioned to maximize the head and neck in the imaging frame and was perpendicular to the sagittal plane. Participants were required to wipe perspiration off the applicable areas prior to measurement using dry wipes. For all measurements, the imaging unit was set to find the hottest point in the frame. Three sequential measurements were performed with the mean used for all analysis.

The STA and PAA temperatures were measured by an Exergen TAT-5000 temporal artery thermometer (Exergen Corporation, Watertown, Massachusetts) using techniques modified from the manual. The TAT-5000 displays the highest temperature recorded during a scan, which consists of a forehead pass from the midline to the hairline followed by a touch on the neck just behind the earlobe. STA and PAA temperatures are highly correlated due to their common source, the internal carotid artery (Williams et al., 2008). Due to potential interference from personal protective equipment, particularly hardhat suspension straps, the two measurements were separated. For the purposes of this study, STA was measured by a forehead pass from the midline to the hairline, whereas PAA was measured by a touch on the neck just behind the earlobe. Participants were required to wipe perspiration off the applicable areas prior to measurement using dry wipes. Three sequential measurements were performed with the mean used for all analysis.

GI temperature was measured by a CorTem HT 150002 ingestible body core sensor (HQ Inc., Palmetto, Florida); data were collected using a CorTemp HT 150016 data recorder (HQ Inc., Palmetto, Florida) and analyzed using CorTrack II data graphing software (HQ Inc., Palmetto, Florida). Research indicates GI sensor temperature readings may be affected by the ingestion of cool liquids for up to 8 h post-ingestion (Goodman et al., 2009; Wilkinson et al., 2008). Therefore, in an effort to avoid the ingestion of food or liquids, but without making participants uncomfortable, study participants were instructed to ingest the sensor the night before monitoring just prior to retiring, and to record the time of ingestion.

Heart rate was measured by a Polar T31 chest transmitter (Polar Electro, Kempele, Finland). Data from the Polar chest belt was collected using a CorTemp HT 150016 data recorder and analyzed using CorTrack II data graphing software.

2.3. Statistical analysis

Statistical analysis was performed using STATA/IC Release 14.1 for Windows (StataCorp LP, College Station, Texas) supplemented with the COCORD module (Cox and Steichen, 2000) to enable calculation of Lin's concordance correlation coefficients and create Bland-Altman plots. Lin's concordance correlation coefficient measures agreement of a continuous measure obtained through two methods by combining measures of precision (r) and accuracy (C_b) in order to determine how far the observed data deviate from the line of perfect concordance (I-Kuei Lin, 1989). The output is a number from -1 to 1 , with perfect positive concordance represented by 1 , perfect negative concordance represented by -1 , and no concordance represented by 0 . As Lin's concordance correlation coefficient is linear in nature, Bland-Altman plots were created to view any non-linear effect. The Bland-Altman method calculates and plots the mean difference between two methods of measurement (bias) and 95% Limits of Agreement (LoA; 1.96 Standard Deviations) against the mean of the two methods of measurement in order to graphically display agreement (Bland and Altman, 1986, 1995, 1999). The 95% LoA are descriptive only. Any interpretation requires establishment of clinically important LoA, which, in this study, was set at ± 0.25 °C and 0.5 PSI to correspond with temperature LoA from other studies (Gunga et al., 2008; Mitchell et al., 2015; Richmond et al., 2015) and PSI LoA equal to twice the temperature LoA as the PSI equation is 50% core temperature.

Analysis consisted of evaluating MFSK, MSSK, STA and PAA for correlation with GI temperature using Lin's concordance correlation coefficient (ρ_c), Pearson's coefficient (r) and the bias correction factor (C_b) along with assessment of measurement agreement using Bland-Altman plots. PSI was calculated by means

of a modified version of the method developed by Moran et al. (1998), along with variations using MFSK, MSSK, STA or PAA in place of GI, as appropriate, based upon agreement in previous analysis. PSI is an index that uses rectal temperature and heart rate to evaluate physiological strain on a universal scale of 0–10 according to the following equation:

$$PSI = 5 \left(\frac{T_{ret} - T_{re0}}{39.5 - T_{re0}} \right) + 5 \left(\frac{HR_t - HR_0}{180 - HR_0} \right) \quad (1)$$

where T_{re0} and HR_0 are rectal temperature and heart rate, respectively, at rest; T_{ret} and HR_t are rectal temperature and heart rate, respectively, at any given point in time. On several occasions employees initiated their work shift prior to checking in with the researchers due to job requirements. As 4 of the 10 participants initiated hot work prior to establishing a baseline GI and HR, and 5 of the remaining 6 participants experienced GI and HR below baseline during recovery, calculation of PSI utilizing Moran's formula was not possible. The cause of elevated baseline GI and HR is unknown, but may have been due to lack of complete recovery from walking from the employee parking lot and climbing 3 flights of stairs to where the self-administered questionnaire was being administered. Due to the lack of a true baseline, the PSI calculation required modification. T_{re0} and HR_0 are used to establish "a universal scale of 0–10 and to overcome the limitations of continually getting higher values during rest or recovery periods" (Moran et al., 1998). The population averages utilized by Moran et al. in the development of PSI (T_{re0} of 36.5 and HR_0 of 60) were used as baseline constants in this study, an approach taken by other researchers (Gaura et al., 2013). This adjustment does not impact PSI within the region of concern ($PSI \geq 7.5$), particularly as the upper limits of $T_{re} = 39.5$ and $HR = 180$ are also population averages rather than individual variables, while the individualized baseline is utilized to prevent negative or elevated PSI values during periods of rest (Moran et al., 1998). Therefore, PSI was calculated using the following equation:

$$PSI = 5 \left(\frac{T_{ret} - 36.5}{3} \right) + 5 \left(\frac{HR_t - 60}{120} \right) \quad (2)$$

3. Results

3.1. Data validation

Data were validated prior to analysis, to include checks on valid values and valid ranges in the recorded data. Data were reviewed visually for physiologically implausible artifacts, such as GI temperature increasing or decreasing by 1.0 °C in a 20-s interval and then quickly returning to previous levels. Measurements outside physiological possibility were deleted and excluded from analysis. During validation it was noted that 2 of the 6 participants with continuously monitored GI showed unexpected temperature effects from fluid consumption despite having ingested the pill > 10 h

Table 2

Concordance, precision and accuracy of measurements in relation to gastrointestinal (GI) temperature. MFSK=Maximum Frontal Skin temperature; MSSK=Maximum Side Skin temperature; STA=Superficial Temporal Artery temperature; PAA=Posterior Auricular Artery temperature; p_{W} = Post-Work; R = Recovery.

Measurement	Lin's CCC (rho_c)	Pearson's (r)	Bias Correction Factor (C_b)
MFSK	0.013	0.074	0.172
MSSK	0.095	0.337	0.269
STA	−0.014	−0.081	0.170
PAA	−0.007	−0.053	0.141
MFSK _{pW}	0.008	0.065	0.119
MSSK _{pW}	0.050	0.190	0.265
STA _{pW}	−0.003	−0.035	0.098
PAA _{pW}	0.015	0.150	0.101
MFSK _R	0.036	0.192	0.188
MSSK _R	0.133	0.496	0.269
STA _R	0.028	0.159	0.178
PAA _R	−0.005	−0.035	0.142

prior to initiating hot work, as recommended by Wilkinson et al. (2008). These temperature effects were identified by reviews of researcher's participant activity logs and a characteristic natural logarithmic recovery curve on the GI temperature plot similar to those presented by Wilkinson et al. (Fig. 1). The presence of this temperature effect extended up to 16-h post-ingestion, a significant finding considering manufacturer's recommendations and the number of subjects affected. Data subject to these interferences were excluded from analysis. Also noted during validation were abnormally low GI temperatures in a single participant during the first 6 h of the shift. Review of the participant's questionnaire and researcher's logs indicated this participant was under treatment for medical conditions and taking prescribed medications with the potential to effect core body temperature. Due to the presence of these conditions the participant was excluded *post hoc*.

3.2. Statistical analysis

MFSK, MSSK, STA and PAA were evaluated for concordance with GI using Lin's concordance correlation coefficient (rho_c), Pearson's coefficient (r) and the bias correction factor (C-b), see Table 2. The results showed no concordance; however, MSSK displayed low precision ($r = 0.337$) and low accuracy ($C_b = 0.269$). Further analysis using data tables, scatterplots and graphs indicated a higher level of concordance during the recovery period following the initial post-work measurement taken upon the participant's return from hot work. Lin's concordance correlation coefficient, Pearson's coefficient and bias correction factor (C-b) were then calculated for initial post-work measurements (MFSK_{pW}, MSSK_{pW}, STA_{pW} and PAA_{pW}) and the remaining recovery measurements (MFSK_R, MSSK_R, STA_R and PAA_R). Initial post-work measurements showed no concordance to GI; however, MSSK_R showed low concordance ($\rho_c = 0.133$), moderate precision ($r = 0.496$) and low accuracy ($C_b = 0.269$) with GI. Further examination of MSSK and GI in

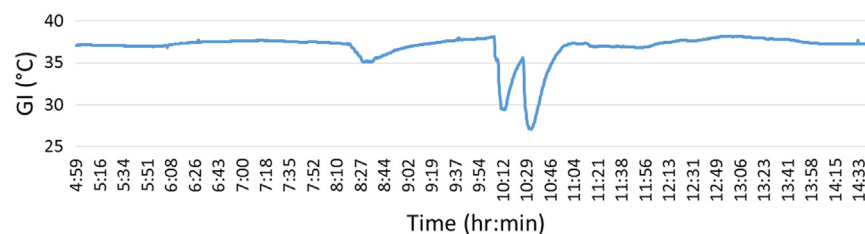


Fig. 1. Gastrointestinal temperature over a work shift. Note the sudden decreases followed by characteristic natural logarithmic recovery curves beginning at 10:04 and ending approximately at 11:00. These decreases correspond to large bolus ingestions of chilled water, highlighting the extent of potential interferences. The less pronounced decrease beginning at approximately 8:15 corresponds with ingestion of a meal.

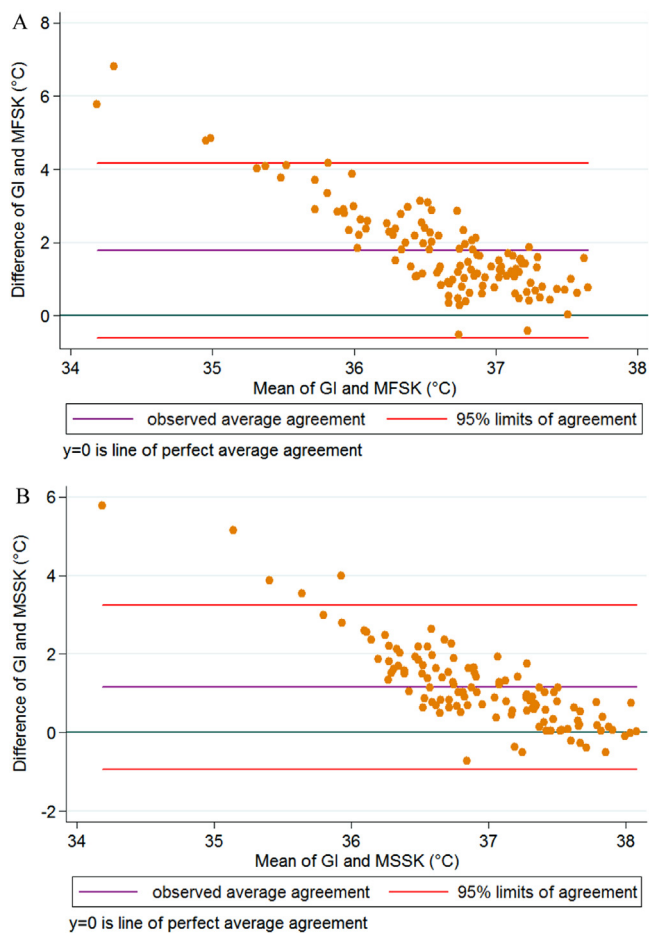


Fig. 2. Bland Altman plots of gastrointestinal temperature (GI) to the following thermal imaging temperatures: (A) Maximum Frontal Skin (MFSK) temperature; (B) Maximum Side Skin (MSSK) temperature.

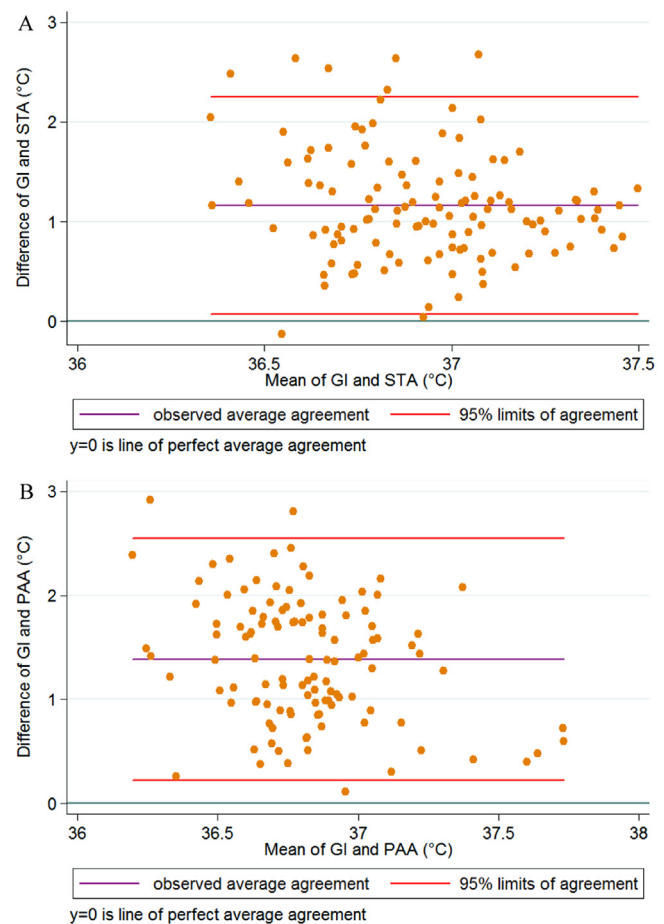


Fig. 3. Bland Altman plots of gastrointestinal temperature (GI) to the following infrared thermometer temperatures: (A) Superficial Temporal Artery (STA) temperature; and (B) Posterior Auricular Artery (PAA) temperature.

relation to time since last heat stress exposure using graphs indicate a diverging trend with increasing time.

In accordance with the common practices of research in the area of core temperature thermography, Bland-Altman plots of MFSK, MSSK, STA and PAA data were generated (Figs. 2A & B, 3A & B). These plots are a common and useful means for determining viability of a measurement as a direct surrogate for another measurement when the true value is not known. Examination of the plots shows increasing agreement between GI and both MFSK and MSSK as core temperature rises. No such agreement was shown between GI and either STA or PAA. Bland-Altman 95% Limits of Agreement (LoA) were large for both MFSK and MSSK at $-0.608, 4.166$ and $-0.927, 3.246$, respectively.

Through separating the measurement data into post-work that is defined as measurements taken upon immediate cessation of hot work, and recovery that is defined as post-work recovery and limiting the analysis of the data to the recovery period for coronal and sagittal views, MFSK_R and MSSK_R LoAs were slightly narrowed to $-0.438, 3.420$ and $-0.559, 2.765$, respectively (Fig. 4A & B). Examination of Bland-Altman plots for these measurements show increasing agreement between both MFSK_R and MSSK_R and GI as core temperature rises, with higher levels of agreement in MSSK_R. Analysis of post-work Bland-Altman plots show a similar trend toward agreement at higher temperatures; however, the agreement was less in post-work measurements compared to recovery measurements. This can be seen by comparing MFSK_{PW} and MSSK_{PW} to MFSK_R and MSSK_R (Figs. 4A & B to 5A & B).

PSI was calculated using GI, MFSK and MSSK in accordance with the modified equation discussed earlier (Eq. (2)). PSI calculated from the alternative temperatures were labeled PSI_{MFSK} and PSI_{MSSK}. Bland-Altman plots for these measurements show a trend toward agreement at higher temperatures, but with generally poor agreement and large LoA (Fig. 6A & B).

4. Discussion

For the period of recovery, the Bland-Altman plots from this study's data display similar agreement to those of Boulari et al. (2012) during recovery. Thermal imagery of the coronal and sagittal views of the head and neck show a general trend toward concordance at higher core body temperatures, although measurement accuracy was not sufficient to allow calculation of individual physiological stress. While several subjects did achieve core temperatures in excess of 38.0°C , calculated PSI reached a high of 5.2 with 83% of observations (99/119) yielding a PSI of <4 . This indicates mild to moderate heat strain in the participants. Boulari et al. identified differences in ambient temperature between exertion and resting phases as a probable cause of lower correlation. In that study the exertion phase was performed in an enclosure heated to $38.8^{\circ}\text{C} \pm 1.0^{\circ}\text{C}$ with $19.2 \pm 2.2\%$ relative humidity to simulate the U. S. Forest Service Pack Test; however, no mechanism of action was proposed.

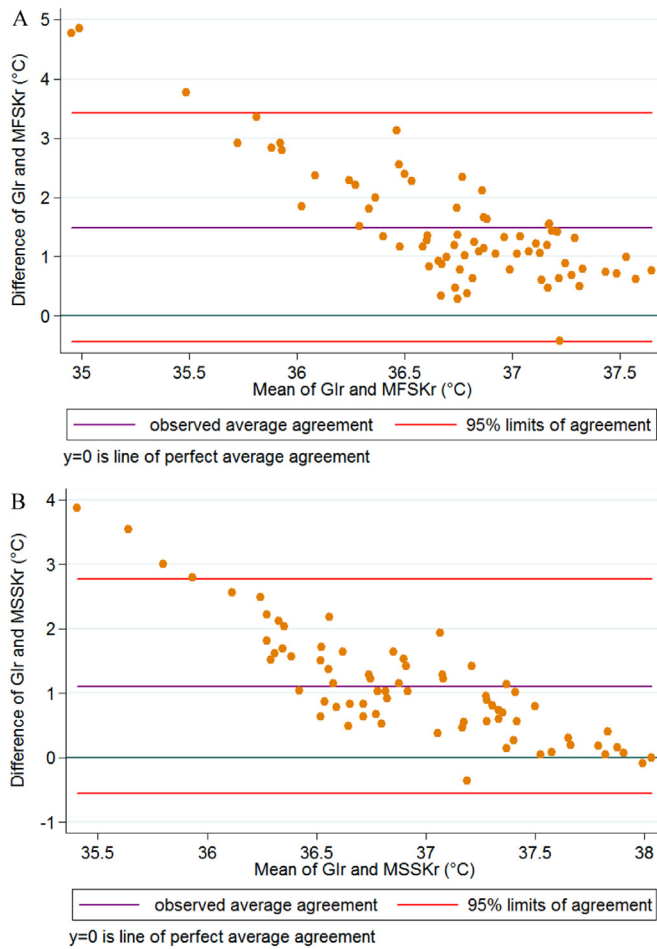


Fig. 4. Bland Altman plots of gastrointestinal temperature (GI) to the following thermal imaging temperatures during recovery: (A) Maximum Frontal Skin temperature (MFSK_R); (B) Maximum Side Skin temperature (MSSK_R).

4.1. Environmental influences

The effect of ambient conditions on thermal imagery is a potential cause for the lack of correlation between GI and both MFSK_{PW} and MSSK_{PW}, along with explaining some variation in MSSK_R. Excess body heat is lost to the environment via evaporation, conduction, convection and radiation. During hot work these losses are minimized due to the encapsulation and insulation provided by PPE. Individuals engaged in hot work therefore experience a microclimate inside of PPE with higher temperatures and humidity, which may drastically increase the wet bulb globe temperature experienced by these individuals, even in mild environmental conditions. Upon doffing PPE, individuals had significant amounts of unevaporated perspiration, which is in equilibrium at the higher WBGT. The initial evaporative effects as this perspiration rapidly phases to a vapor may have reduced skin temperatures enough to effect readings. Participants towed dry prior to measurement, however, at moderate levels of heat strain perspiration continued for a significant period after exposure. This may result in both continued evaporative effects and variations in emissivity due to the surface film of sweat. Ambient temperatures ranging from 20 to 23 °C were observed in the recovery area compared to the 38.8 °C ± 1.0 °C in the [Bourlai et al. \(2012\)](#) heated enclosure. The larger temperature gradient experienced during recovery can be expected to increase conductive, convective and radiative heat losses. These heat losses are unlikely to be uniform and thereby may contribute to the observed variation of agreement between measurements, as hypothesized by [Boulari et al.](#)

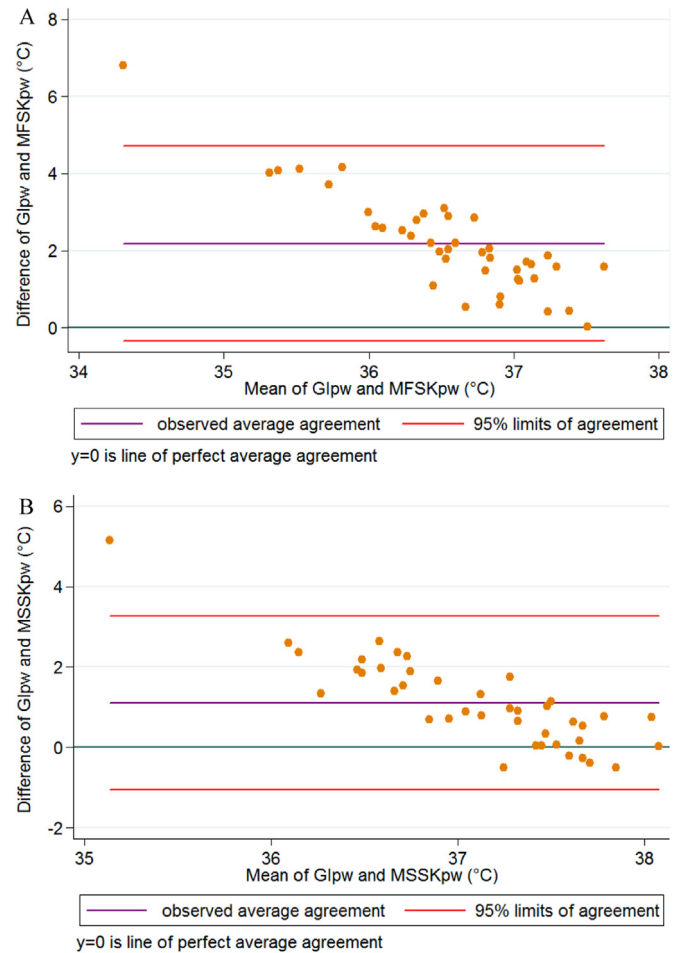


Fig. 5. Bland Altman plots of gastrointestinal temperature (GI) to the following thermal imaging temperatures immediately post-work: (A) Maximum Frontal Skin temperature post-work (MFSK_{PW}); and (D) Maximum Side Skin temperature post-work (MSSK_{PW}).

Supporting the hypothesis that environmental influences are affecting thermal imagery measurements at a time when temperatures would be expected to be nearer agreement with core temperatures is the time dependent increasing divergence of GI and thermal imagery temperatures during recovery. Given this trend, one would expect an increased agreement for the measurement taken immediately post-work. Additional evidence can be seen in other studies that have identified insulation effects as increasing correlation between skin and core temperatures ([Mitchell et al., 2015](#); [Pryor et al., 2011](#); [Richmond et al., 2015, 2013](#)).

Regarding variation in MSSK_R, the primary location of the hottest sagittal point was typically the ear canal. Considering the protection afforded by both the external pinna and ear canal, one would anticipate a lower level of environmental influence. However, variation among the location of the automatically selected hot spots was noted. The location migrated between the internal acoustic meatus, intertragic notch and tragus. The location appeared dependent upon depth of line-of-sight penetration into the internal acoustic meatus, with deeper penetration yielding higher temperatures. This variation appeared dependent on individual anatomical variation and camera angle as influenced by body habitus.

4.2. Cool fluids and effects on GI sensor temperature

Two of the 6 continuously monitored participants in the study displayed significant effects on the sensor measured temperature

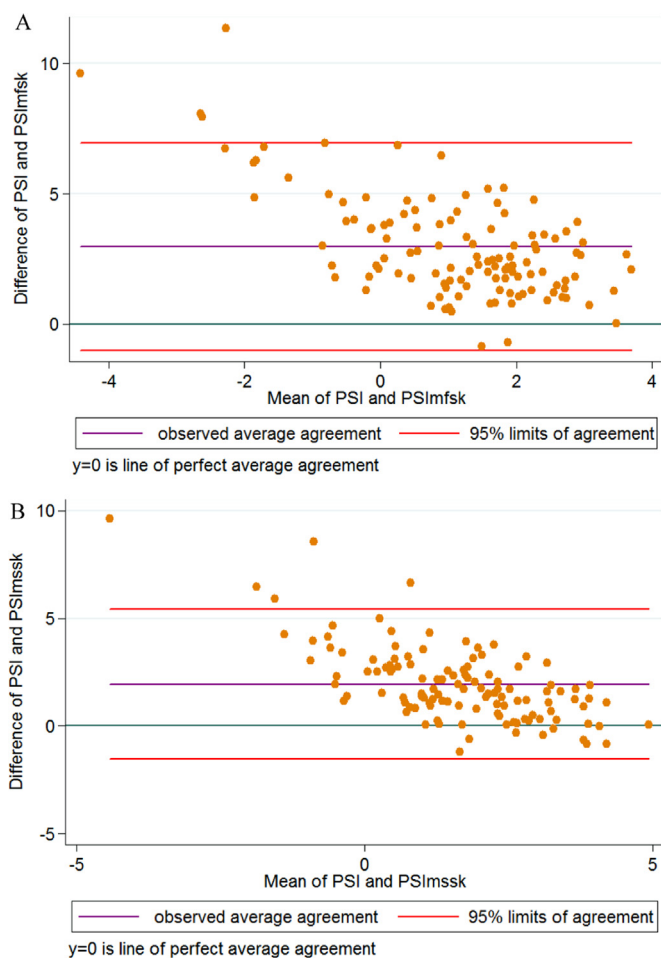


Fig. 6. Bland Altman plots of PST to: (A) PSI calculated using Maximum Frontal Skin (MFSK) temperature (PSI_{MFSK}) and (B) PSI calculated using Maximum Side Skin (MSSK) temperature (PSI_{MSSK}).

from ingestion of cool liquids. Subjects ingested the sensors at 7:00 PM the night prior and ingestion was verified with researchers via text message contact at 7:30 PM, as previously arranged. While gastrointestinal motility is highly variable, manufacturer instructions suggest ingestion time of 2 h pre-monitoring and previous research has recommended ingestion 10 h prior to monitoring in order to reduce interference due to ingestion of chilled water (5–8 °C) (Wilkinson et al., 2008).

Fig. 1 displays gastrointestinal temperature over a work shift for one of the affected participants. The sudden drops followed by characteristic natural logarithmic recovery curves beginning at 10:00 and ending approximately at 11:00 correspond to post-work intakes of chilled water and are similar to those previously reported in a study of the effect of chilled water on GI sensor temperature (Wilkinson et al., 2008). The less pronounced dip beginning at 8:15 corresponded with ingestion of a meal. This interference highlights the need to closely monitor food and drink intake during all monitoring utilizing GI sensors.

4.3. Strengths

Participants working in a real-world occupational setting were evaluated, which is in contrast to the laboratory setting of Boulari et al. Additionally, the participants were more representative of the United States worker population in age and BMI than most heat stress and heat strain studies, many of which are sponsored by the United States Department of Defense and evaluate military

combat personnel who are generally younger and in better physical condition.

4.4. Limitations

In comparison to Boulari et al. and other studies, the primary cause of heat stress in this study is infrared radiation rather than metabolic load. High levels of infrared radiation may cause localized heating of the skin and immediate subsurface without immediate effects on core temperature, a possible contribution to the variability observed in immediate post-work measurements. After a tapping procedure was completed, the participants stepped away from the furnace to areas of low infrared radiation for a significant period of time to evaluate molten flow, which theoretically decreased the effect of localized heating prior to participant temperature measurement. As the level of infrared radiation was not measured, this potential effect could not be confirmed nor quantified.

In contrast to the Fluke thermal imaging unit, Boulari et al. utilized a mid-wave infrared thermal imager from FLIR Systems, Inc. (Wilsonville, OR) with indium antimonide micobolometers in a 1024 × 1024 focal plane array yielding a thermal sensitivity of ≤ 0.025 °C in the 3–5 μm spectral band. Variation due to the use of the 8–14 μm versus the 3–5 μm spectral band is considered insignificant as both are common infrared imaging windows selected to avoid infrared absorption at 6.3 μm due to water vapor. Additionally, Boulari et al. calculated the estimated maximum temperature in a manually selected region of interest, with each frame's region of interest to contain, on average, approximately 160,000 pixels (2012). The estimated maximum temperatures derived from the first 50 frames were then averaged to yield the estimated core temperature. The combination of manual selection, higher resolution, higher thermal sensitivity and averaging over 50 frames would be expected to display less measurement variability compared to the automatic hot spot detection used in this study. It is unknown if measurements performed in this method achieve statistically higher correlation to true skin temperatures. The greater number of pixels increases resolution of image, however, this increased resolution may not necessarily result in increased measurement precision or accuracy.

In this study the researchers noted several instances of the Fluke Ti45FT-10/20 thermal imaging unit performing a self-initiated recalibration. Measurements taken immediately prior to the recalibration procedure were lower than those immediately after recalibration. As recalibration times were random, occurring both between participants, between consecutive measurement sets of the same participant and sequential measurements of the same participant, no adjustments were made to the data. Recalibration was noted to raise the measured temperature and thermal imaging temperatures were consistently lower than gastrointestinal temperatures, thus any instrument effect would decrease correlation. Therefore, the true correlation of MSSK_R to GI is potentially higher than observed.

4.5. Future research directions

The ear canal shows promise as a measurement site for core body temperature given observations during measurement, particularly if adequately insulated from environmental influences. While we recorded low correlation, moderate precision and low accuracy in comparison with GI, much of the observed variation is hypothesized to be dependent on individual anatomical variation and camera angle influenced by body habitus. As indicated by Taylor et al. (2014) in their review article, core-to-shell and ambient-to-skin temperature gradients must be minimized using zero-gradient instruments in order to accurately measure core

temperature at the surface. Due to high tissue perfusion and the cavity configuration of the ear canal, it appears well suited for a purpose designed zero-gradient instrument to achieve continuous temperature monitoring.

5. Conclusions

Results of this study confirmed previous research (Bourlai et al., 2012) showing thermal imagery is not highly correlated to body core temperature during recovery from moderate heat strain in mild ambient conditions. Measurements display a trend toward increasing correlation at higher body core temperatures which may enable use of thermal imagery as a screening tool for high heat strain; however, accuracy is not sufficient at mild to moderate heat strain to allow calculation of individual physiological stress.

Due to worker PPE requirements, evaluation of the accuracy of thermal imagery during work was not feasible. Further development of the method may yield useful measures of core body temperature during work and/or under specific conditions.

Acknowledgments

Funding: This work was supported by the National Institute of Occupational Safety and Health of the National Institutes of Health [award number T42OH008414–10] [grant number T42/CCT810426].

The authors would like to thank the copper smelter management and employees for their participation in this study. Additionally, special thanks to Ms. Tracy Rees, MFA, Technical Writer, for reviewing and revising the research document.

References

- American Conference of Governmental Industrial Hygienists, 2015. TLVs and BEIs. ACGIH Signature Publications, Cincinnati.
- Arbury, S., Jacklitsch, B., Farquah, O., Hodgson, M., Lamson, G., Martin, H., Proffitt, A., Office of Occupational Health Nursing, O.S., Health, A., 2014. Heat illness and death among workers - United States, 2012–2013. *Morbidity and Mortality Weekly Report*, pp. 661–665.
- Bland, J.M., Altman, D., 1986. Statistical methods for assessing agreement between two methods of clinical measurement. *Lancet* 327, 307–310.
- Bland, J.M., Altman, D.G., 1995. Comparing methods of measurement: why plotting difference against standard method is misleading. *Lancet* 346, 1085–1087.
- Bland, J.M., Altman, D.G., 1999. Measuring agreement in method comparison studies. *Stat. Methods Med. Res.* 8, 135–160.
- Bourlai, T., Pryor, R.R., Suyama, J., Reis, S.E., Hostler, D., 2012. Use of thermal imagery for estimation of core body temperature during precooling, exertion, and recovery in wildland firefighter protective clothing. *Prehospital Emerg. Care* 16, 390–399.
- Cox, N. J., & Steichen, T. (2000). CONCORD: Stata module for concordance correlation. *Statistical Software Components*. Boston College Department of Economics. Retrieved from <https://ideas.repec.org/c/boc/bocode/s404501.html>.
- Gaura, E., Kemp, J., Brusey, J., 2013. Leveraging knowledge from physiological data: on-body heat stress risk prediction with sensor networks. *IEEE Trans. Biomed. Circuits Syst.* 7, 861–870.
- Goodman, D.A., Kenefick, R.W., Cadarette, B.S., Cheuvront, S.N., 2009. Influence of sensor ingestion timing on consistency of temperature measures. *Med. Sci. Sports Exerc.* 41, 597–602.
- Gunga, H.C., Sandsund, M., Reinertsen, R.E., Sattler, F., Koch, J., 2008. A non-invasive device to continuously determine heat strain in humans. *J. Therm. Biol.* 33, 297–307.
- I-Kuei Lin, L., 1989. A concordance correlation coefficient to evaluate reproducibility. *Biometrics* 45, 255–268.
- Mitchell, J.B., Goldston, K.R., Adams, A.N., Crisp, K.M., Franklin, B.B., Kreutzer, A., Montalvo, D.X., Turner, M.G., Phillips, M.D., 2015. Temperature measurement inside protective headgear: comparison with core temperatures and indicators of physiological strain during exercise in a hot environment. *J. Occup. Environ. Hyg.* 12, 866–874.
- Moran, D.S., Shitzer, A., Pandolf, K.B., 1998. A physiological strain index to evaluate heat stress. *Am. J. Physiol.* 275, R129–R134.
- Nagano, C., Tsutsui, T., Monji, K., Sogabe, Y., Idota, N., Horie, S., 2010. Technique for continuously monitoring core body temperatures to prevent heat stress disorders in workers engaged in physical labor. *J. Occup. Health* 52, 167–175.
- Parsons, K.C., 1999. International standards for the assessment of the risk of thermal strain on clothed workers in hot environments. *Ann. Occup. Hyg.* 43, 297–308.
- Pryor, R.R., Seitz, J.R., Morley, J., Suyama, J., Guyette, F.X., Reis, S.E., Hostler, D., 2011. Estimating core temperature with external devices after exertional heat stress in thermal protective clothing. *Prehospital Emerg. Care* 16, 136–141.
- Richmond, V.L., Davey, S., Griggs, K., Havenith, G., 2015. Prediction of core body temperature from multiple variables. *Ann. Occup. Hyg.* 59, 1168–1178.
- Richmond, V.L., Wilkinson, D.M., Blacker, S.D., Horner, F.E., Carter, J., Havenith, G., Rayson, M.P., 2013. Insulated skin temperature as a measure of core body temperature for individuals wearing CBRN protective clothing. *Physiol. Meas.* 34, 1531–1543.
- Taylor, N.A.S., Tipton, M.J., Kenny, G.P., 2014. Considerations for the measurement of core, skin and mean body temperatures. *J. Therm. Biol.* 46, 72–101.
- Wilkinson, D.M., Carter, J.M., Richmond, V.L., Blacker, S.D., Rayson, M.P., 2008. The effect of cool water ingestion on gastrointestinal pill temperature. *Med. Sci. Sports Exerc.* 40, 523–528.
- Williams, E.M., Heusch, A.I., McCarthy, P.W., 2008. Thermal screening of facial skin arterial hot spots using non-contact infrared radiometry. *Physiol. Meas.* 29, 341–348.